Title	Tailoring asymmetric discharge-charge rates and capacity limits to extend Li-O2 battery cycle life
Authors	Geaney, Hugh;O'Dwyer, Colm
Publication date	2017-01-27
Original Citation	Geaney, H. and O'Dwyer, C. (2017) 'Tailoring asymmetric discharge-charge rates and capacity limits to extend Li-O2 battery cycle life', ChemElectroChem, 4, pp. 628-635. doi:10.1002/celc.201600662
Type of publication	Article (peer-reviewed)
Link to publisher's version	10.1002/celc.201600662
Rights	© 2017, John Wiley & Sons, Inc. This is the peer reviewed version of the following article: Geaney, H. and O'Dwyer, C. (2017) 'Tailoring asymmetric discharge-charge rates and capacity limits to extend Li-O2 battery cycle life', ChemElectroChem, 4, pp. 628-635. doi:10.1002/celc.201600662, which has been published in final form at http://dx.doi.org/10.1002/celc.201600662 This article may be used for non-commercial purposes in accordance with Wiley Terms and Conditions for Self-Archiving.
Download date	2024-05-05 19:40:07
Item downloaded from	https://hdl.handle.net/10468/4417

Accepted Article

Title: Tailoring Asymmetric Discharge-Charge Rates and Capacity Limits to Extend Li-O2 Battery Cycle Life

Authors: Hugh Geaney and Colm O'Dwyer

A Journal of

ChemPubSoc
Europe

WILEY-VCH   www.chemelectrochem.org

FULL PAPER

Tailoring Asymmetric Discharge-Charge Rates and Capacity Limits to Extend Li-O$_2$ Battery Cycle Life

Hugh Geaney[a],[b], and Colm O'Dwyer[a],[c]*

Abstract: Widespread issues with the fundamental operation and stability of Li-O$_2$ cells impact cycle life and efficiency. While the community continues to research ways of mitigating side reactions and improving stability to realize Li-O$_2$ battery prospects, we show that limiting the depth-of-discharge while unbalancing discharge/charge rate symmetry can extend Li-O$_2$ battery cycle life by ensuring efficient reversible Li$_2$O$_2$ formation, markedly improving cycle life. Systematic variation of the discharge/charge currents shows that clogging from discharging the Li-O$_2$ cell at high current (250 µA) can be somewhat negated by recharging with a lower applied current (50 µA), with a marked improvement in cycle life achievable. Our measurements determined that specific reduction of the depth of discharge in decrements from equivalent capacities of 1000 mAhg^{-1} to 50 mAhg^{-1} under symmetric discharge/charge currents of 50 µA strongly affected the cumulative discharge capacity of each cell. A maximum cumulative discharge capacity was found to occur at ~10 % depth of discharge (500 mAhg^{-1}) and the cumulative discharge capacity of 39,500 mAhg^{-1} was significantly greater than cells operated at higher and lower depths of discharge. The results emphasize the importance of appropriate discharge/charge rate and depth of discharge selection for other cathode/electrolyte combinations for directly improving cycle life performances of Li-O$_2$ batteries.

[a]   Dr H. Geaney, Dr C. O'Dwyer
       Department of Chemistry, University College Cork, Cork,
       T12 YN60, Ireland
       *Email: c.odwyer@ucc.ie

[b]   Dr H. Geaney
       Present address: Materials & Surface Science Institute, University of
       Limerick, Limerick, Ireland

[c]   Dr C. O'Dwyer
       Micro-Nano Systems Centre, Tyndall National Institute, Lee
       Maltings, Cork, T12 R5CP, Ireland

       Supporting information for this article is given via a link at the end of
       the document.

Introduction

Li-O$_2$ batteries have been widely investigated as 'post Li-ion' energy storage solutions due to the high theoretical specific energy of the Li-O$_2$ system.[1-6] Despite the immense potential of Li-O$_2$ batteries to revolutionize energy storage for demanding applications (e.g. in the automotive industry), a number of significant issues have been identified which must be addressed if Li-O$_2$ systems are to become realistic practical replacements for existing Li-ion batteries.[7-11] These issues encompass a wide range of problems from electrode (anode and cathode) and electrolyte instabilities to system architecture and poor rate capabilities.[12, 13] Fundamentally, enhanced rechargeability is a prerequisite for the system as only a small number of studies have shown Li-O$_2$ batteries with cycle lifetimes of ≥ 100 at deep discharge.[12, 14] Recent efforts have focused on developing a greater understanding of the battery chemistry occurring during discharge and charge.[15-19] The overall discharge/charge mechanism for Li-O$_2$ batteries involves the reversible formation and decomposition of Li$_2$O$_2$.[20, 21] However, an increasingly complex picture has emerged of the influence of a plethora of factors on battery chemistry. This is particularly important as the chemistry, size, crystallinity, and location of the discharge products within the cathode will all influence the rechargeability of the battery.[22-24] The electrolyte solvent in particular has been shown to strongly influence the discharge mechanism with the Gutman donor and acceptor numbers (DN and AN respectively) giving insight into whether a solution or surface based growth mechanism will dominate.[25] TEGDME, DME and DMSO are the most commonly used electrolyte solvents in Li-O$_2$ cells that have shown a degree of stability (i.e. ability to form Li$_2$O$_2$ over an extended number of cycles without immediate electrolyte decomposition). The two former electrolyte solvents possess lower DN and AN values than DMSO, meaning that for a given cathode architecture, DMSO discharges tend to form much larger discharge product feature sizes, leading to higher discharge capacities.[26]

The depth of discharge is a crucial consideration for Li-O$_2$ batteries systems. It has been widely shown that the primary failure mechanisms for Li-O$_2$ batteries involve the accumulation of by-products formed by side reactions between Li$_2$O$_2$ (and its intermediates) and the electrolyte and cathode.[27-31] These side reactions are particularly problematic at high charging voltages and become more pronounced as cycle number increases.[32] This issue has prompted researchers to operate Li-O$_2$ batteries at less than full depths of discharge to minimize high voltage charging and extend cycle life. Given the issues with conducting tests at full depth of discharge, the majority of reported literature studies focus on cycling at a fixed capacity value (routinely 1000 mAhg^{-1} $_{carbon}$).[33-37] This approach may allow the impact of side-reactions to be partially alleviated because the voltage to which the battery is charged is often much less than when tests are conducted at full depth of discharge. Despite this, the full

FULL PAPER

discharge capacity of Li-O_2 battery cathodes can vary considerably based on their chemistry, architecture, applied current and the chosen electrolyte composition. This means that it is often difficult to gauge how the % depth of discharge is represented by a capacity limit of 1000 mAhg^{-1}, and (unless it is explicitly stated) what process is the cause of limited performance. This factor was recently emphasized with practical examples by Noked et al. who discussed the influence of depth of discharge (along with current collector choice, mass loading and other important practical considerations) and highlighted its importance in assessing practical Li-O_2 systems.[37]

It has often been stated that 'sluggish' kinetics for oxygen evolution reaction (OER) during charge are a major hurdle for the implementation of Li-O_2 batteries.[38-40] This perhaps explains why the rate capabilities of Li-O_2 batteries have been more sparingly assessed than those of Li-ion batteries.[41, 42] Instead, a number of studies have focused on the current dependent formation of Li$_2$O$_2$ in different electrolyte and cathode permutations as a measure of understanding rate dependent operation (i.e. for faster discharge behaviour). Adams et al. showed that Li$_2$O$_2$ formation on Super P cathodes in a TEGDME electrolyte was strongly current dependent with large toroids only forming at lower current densities.[43] They also presented a large influence of asymmetric discharging and charging currents (i.e. discharge at high current and charge at low current and vice versa) on the charging overpotential (the potential difference between 2.96 V and the observed charging potential) but did not assess the impact of this asymmetry on cycle life. Asymmetric discharge and charge currents may be a means of extending cycle life by finding compatible discharge/charge current ratios that drive a minimization of charge overpotentials and thus alleviate side reactions for extended cycling without prescribed catalyst or sacrificial/redox mediator salt addition to the cathode or electrolyte. Unbalancing the discharge and charge rates may, as we will show here, improve cyclability in cases where the carbon cathode contains a lot of discharge product. Furthermore, asymmetric discharge/charge rates may actively be desired by manufacturers for certain applications (e.g. in cell phones where fast charges and slow discharge rates are advantageous) and fundamentally, it provides a means of assessing how the discharge state and product type and morphology can be effectively decomposed to maximize cycle life, for a predetermined capacity limit and energy density.

In this report we investigate the influence of discharge/charge asymmetry in determining the rechargeability of a fixed cathode/electrolyte pairing (DMSO/LiTFSI electrolyte and carbon nanotube (CNT)/ Poly(ethylene oxide) (PEO) cathode). The electrolyte was chosen as it facilitates higher discharge capacities (despite not exhibiting acceptable stability for practical applications[44]) than ether based electrolytes.[45-48] CNTs have been shown to possess higher discharge capacities than particulate carbon while also allowing easier identification of discharge products.[48-52] PEO was utilized as a more stable cathode binder compared to the more widely used PVDF.[53] It must be stressed that this report is not proposing this electrolyte/cathode pairing as a truly stable Li-O_2 system which would be feasible for practical applications. Instead, tests were done in the context of recent literature focus on understanding the influence of different testing protocols on determining the electrochemical response of Li-O_2 systems.[54] The impact of high

(250 µA), medium (100 µA) and low (50 µA) applied discharge and charge currents on determining cycle life for a fixed depth of discharge (1000 mAhg^{-1}) is first investigated. We also assess the influence of depth of discharge for a fixed discharge/charge current (symmetric ±50 µA) on determining the total cumulative discharge capacity by varying the depth of discharge from full depth of discharge (when cycled between 2.0 → 4.5 V) to extremely low depth of discharge (50 mAhg^{-1}). The report suggests that a depth of discharge of ~10% results in the largest cumulative cell discharge capacity and also highlights that discharge/charge asymmetry may be a useful means of reducing charge overpotential and increasing cycle life.

Results and Discussion

Since many literature reports limit the discharge capacity to 1000 mAhg^{-1} during cycling, we first investigated the nature of discharge products formed on the CNT cathodes as a function of applied current (Figure 1). Such capacity limits are used in Li-O_2 battery analysis instead of a voltage, in order to define a depth of discharge. However, what we will demonstrate as part of this investigation is that the depth of discharge is also precariously defined by a capacity limit, as it is for a voltage for the ORR process of Li$_2$O$_2$ formation during discharge. SEM images confirm that the CNT cathodes show obvious discharge product formation across the surface and within the nanotube network.
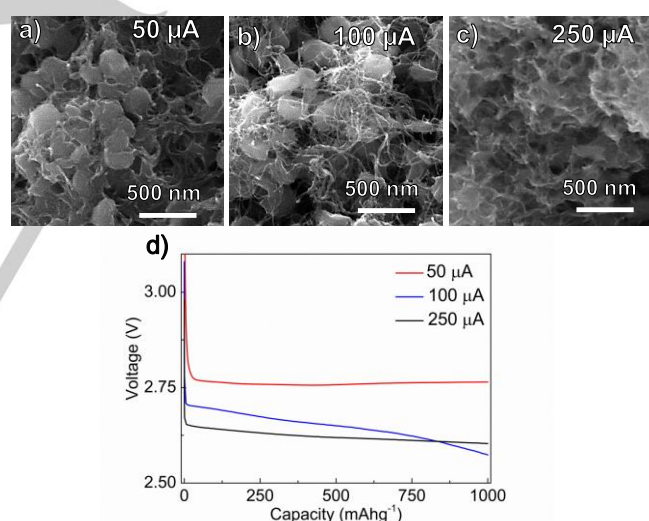

Figure 1. SEM images of CNT cathodes discharged in DMSO electrolyte to a depth of discharge of 1000 mAhg^{-1} at with different applied currents (a,b: 50 µA c,d: 100 µA e,f: 250 µA) and corresponding discharge profiles (g).

The sub-µm sized discharge products seen at 50 µA and 100 µA are consistent with those previously seen for a DMSO based electrolyte on a particulate carbon cathode.[44, 55] Despite the clear presence of spherical/toroidal particles across the surface, the underlying CNT support is still clearly visible (see Figure S1 for SEM images of a pristine CNT cathode). In contrast, the cathode discharged at 250 µA showed slightly less morphologically defined discharge products (i.e. the toroidal shape was not as obvious) consistent with the current dependent

FULL PAPER

size of discharge products widely reported.[56, 57] From the corresponding discharge profiles, we observe that the discharge potential for the cathode discharged at 50 µA is markedly higher than at higher discharge rates (100 µA, 250 µA).

Discharge/charge tests were conducted to a fixed discharge capacity of 1000 mAhg^{-1} using high (250 µA), medium (100 µA) and low currents (50 µA) in each of the nine possible symmetric and asymmetric charging-discharge permutations. The first ten cycles are shown for comparison for each of the nine permutations of charging and discharging at 250 uA, 100 µA and 50 µA are shown in Figure 2.
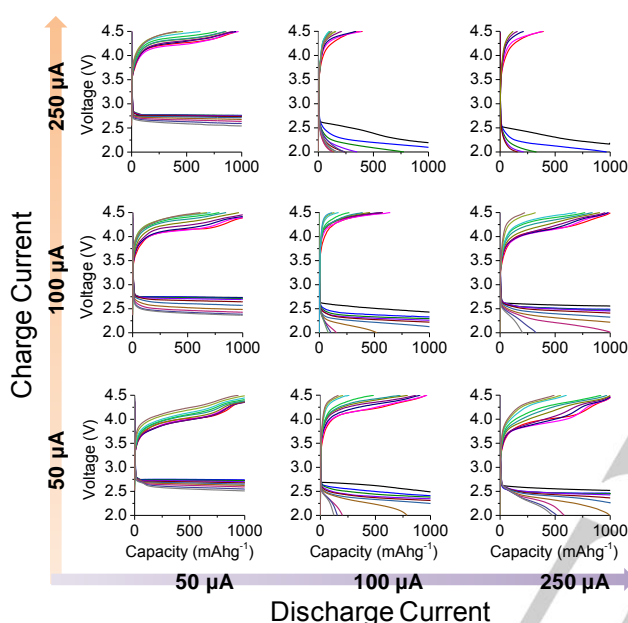

Figure 2. First ten discharge/charge cycles to a capacity of 1000 mAhg^{-1} for various symmetric and asymmetric discharge/charge currents.

It can clearly be seen that the test conducted symmetrically at ± 250 µA showed poor rechargeability and only maintained a discharge capacity of 1000 mAhg^{-1} for 1 cycle due to the extremely poor charging behaviour (even the first charge failed to reach 1000 mAhg^{-1} before the upper voltage limit of 4.5 V was reached). The discharge capacity rapidly dropped off and was <500 mAhg^{-1} by the third cycle. In contrast, a marked improvement can be seen when the tests were operated under asymmetric conditions. For the cells charged at 100 µA and 50 µA, there is an obvious improvement in capacity retention reflected in greatly improved charging behaviour. The discharge and charge capacities for the tests presented in Figure 2 will be compared with the other asymmetric tests discussed in terms of cycle life (Figure 3) and charge overpotential (Figure 4). The first charging profiles for each of the tests discharged at 250 µA are also shown in Figure S2) for comparison. It can clearly be seen that the charging overpotential increases in the order of 50 µA < 100 µA < 250 µA.

Similar tests but with a discharge current of 100 µA and charge currents of 250 µA, 100 µA and 50 µA are presented in

Figure 2. Similar to the behaviour from discharge at 50 µA, the test with a charge current of 250 µA immediately showed an extremely large charge overpotential and was not able to achieve a first charge capacity of 1000 mAhg^{-1}. The symmetric ± 100 µA test showed improved discharge capacity retention (6 discharge cycles to 1000 mAhg^{-1}) despite not achieving a single full capacity charge at 4.5 V or lower. Charging at 50 µA led to an obvious improvement in charging with significant reduction in charge overpotential and level of charge (i.e. charging to a higher capacity), but no improvement in the number discharge cycles. Despite this, the first incomplete discharge capacity for this test (≈ 750 mAhg^{-1}) was higher than that measured for the symmetric (± 100 µA) test (≈500 mAhg^{-1}). The first charge profile comparison for each of the tests (Figure S3) again showed a large improvement for the test at 50 µA compared to the others with a much larger charge capacity at lower voltages.

Further reduction of the discharge current to 50 µA was also probed as a means of improving capacity retention. Even for a five-fold increase in charging rate (charge current of 250 µA), the capacity retention was markedly improved compared to the tests at higher discharge currents. In fact, all of the tests with a discharge current of 50 µA could retain a capacity of 1000 mAhg^{-1} for more than ten cycles when recharged at the same rate, or charged up to five times faster. What can clearly be seen in these tests is that the charging behaviour improved from 250 µA to 100 µA and was best after charging at 50 µA. This improved behaviour is manifested in the reduced charge overpotential seen in the first cycles from 250 µA to 100 µA and 50 µA (Figure S2). The first charge profiles for each of the charge currents are also presented in Figure S3. One means of further improving performance/reducing the impact of side reactions may be through the use of potentiostatic segments in charging (i.e. setting charging potential at a fixed held upper potential limit beyond which side-reactions are known to dominate). This possibility is discussed in depth with an example in Figure S4 and will be the subject of further investigations in future.

Capacity retention/cycle life summaries for the various tests limited to capacities of 1000 mAhg^{-1} are presented in Figure 3. The tests are grouped according to common discharge current. Figure 3 a) shows the cells with discharge currents of 50 µA while Figure 3 b) and c) show the tests with discharge currents of 100 µA and 250 µA respectively. Cells discharged with an applied current of 50 µA (Figure 3 a), all delivered >10 discharge cycles. Increasing the charge current had a minor influence on cycle life (i.e. incrementing the charge rate from 50 µA to 250 µA resulted in a loss of just 3 cycles). For the tests discharged at 100 µA (Figure 3 b), the impact of charge current was more pronounced with only two cycles possible when charged at 250 µA. Similarly, poor rechargeability was seen for cells discharged symmetrically at 250 µA (Figure 3 c). Interestingly, the cycle life of the other 250 µA discharge tests with asymmetric, slower charge currents of 50 and 100 µA showed an impressive 7 and 8 cycles respectively. This suggests that improved cycle life performance may be achievable for other capacity-limited Li-O$_2$ battery systems if high discharge currents are offset by slower recharge rates.
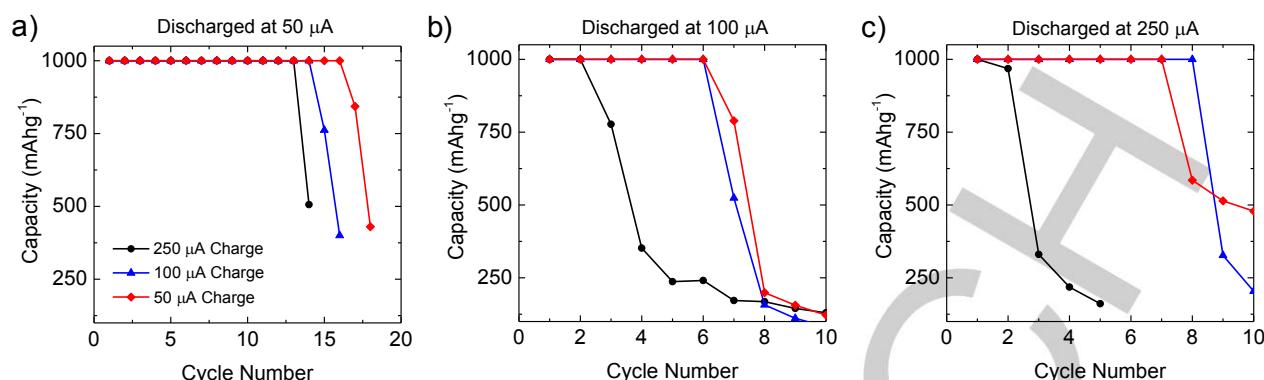
FULL PAPER

Figure 3. Summary of discharge capacity retention for the test shown in Figures 2-4. The discharge capacity for each cycle is shown for cells discharged at a) 50 µA, b) 100 µA, c) 250 µA.

At full depth of discharge to 2 V, the total discharge capacity decreased as a function of increased applied current with Figure 4 a) 250 µA ($\approx$2800 mAhg^{-1}), Figure 4 b) < 100 µA ($\approx$3950 mAhg^{-1}), Figure 4 c) < 50 µA ($\approx$4450 mAhg^{-1}). These discharge capacities are larger than the majority of capacities previously reported for cathodes based on particulate carbons (i.e. Super P and Ketjen black) and are particularly high given that the current collector used here was chosen so that it does not participate in, nor contribute to, the cell discharge and overall capacity.[58-60]

Figure 4. Discharge profiles and corresponding SEM image for CNT cathodes discharged at a,b) 50 µA, c,d) 100 µA, e,f) 250 µA.

In contrast to the tests performed at limited discharge, SEM analysis of the cathodes after a single full discharge showed much greater amounts of discharge products with the underlying CNTs almost completely obscured in the SEM images (Figure 4 d-f). This complete coverage with discharge products may explain why rechargeability at full depth was so limited (Figure S5) and is consistent with previous studies where full depths of discharge have led to large discharge product deposits and poor rechargeability.[25, 56, 57]

Based on the observation that tests conducted under symmetric discharge/charge conditions of ± 50 µA provided the largest number of cycles, the influence of depth of discharge on the total cumulative discharge capacity was also investigated. This was done by varying the depth of discharge to 1000 mAhg^{-1}, 750 mAhg^{-1}, 500 mAhg^{-1}, 250 mAhg^{-1}, 80 mAhg^{-1} and 50 mAhg^{-1}. SEM images of the cathodes after single discharges at each of these discharge depths are presented in Figure S6 and S7 while examples of discharge/charge profiles at selected cycle numbers are provided in Figure S8.

The number of discharge cycles from the Li-O$_2$ battery can be considerably increased by controlling the reduction in the depth of discharge as shown in Figure 5 a). For example, the cell cycled at a depth of discharge of 1000 mAhg^{-1} achieved 16 cycles while the cell cycled at 50 mAhg^{-1} achieved 556 coulombically equivalent cycles. The data can be fitted quite well qualitatively with an exponential decay function, thus providing a predictor for cycle life depending on the capacity limit for this or other Li-O$_2$ systems. The total achievable discharge capacity at each of the investigated discharge depths is presented in Figure 5 b). It can be seen that the smallest cumulative discharge capacity of 10,397 mAhg^{-1} was recorded at full depth of discharge (i.e. when tests were conducted between 2.0-4.5 V as seen in Figure S5). This finding is to be expected as this limited rechargeability at full depth of discharge is what has influenced the majority of literature reports to use a fixed 1000 mAhg^{-1} capacity limit.[60] Limiting the discharge capacity to 1000 mAhg^{-1} led to a total discharge capacity of 16,000 mAhg^{-1} for all cycles combined. This achievable discharge capacity increased to 19,250 mAhg^{-1} at a 750 mAhg^{-1} and reached a maximum total specific capacity of 39,500 mAhg^{-1} at a discharge limit of 500 mAhg^{-1}, which corresponds to a Li-O$_2$ battery that provides a specific energy of ~1.4 kWh kg^{-1} consistently each cycle for over 100 cycles. This suggests that the maximum total discharge capacity for this
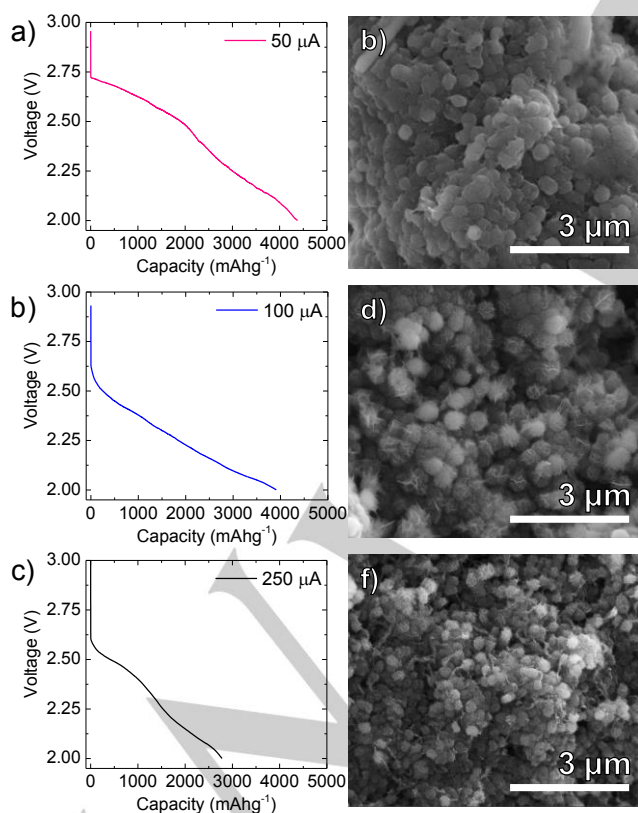
FULL PAPER

electrolyte/cathode pairing is provided at approximately 10% of total depth of discharge (i.e. at 500 mAhg^{-1}), corresponding to a cell discharge voltage of 2.75 V in this case. Interestingly, total discharge capacity decreased slightly at lower depths of discharge (i.e. 250 mAhg^{-1} and 50 mAhg^{-1} yielded total discharge capacities of 30,250 mAhg^{-1} and 27,800 mAhg^{-1} respectively) suggesting that the fundamental instability of the discharge/charge chemistry in this cell cannot simply be circumvented by reducing depth of discharge.
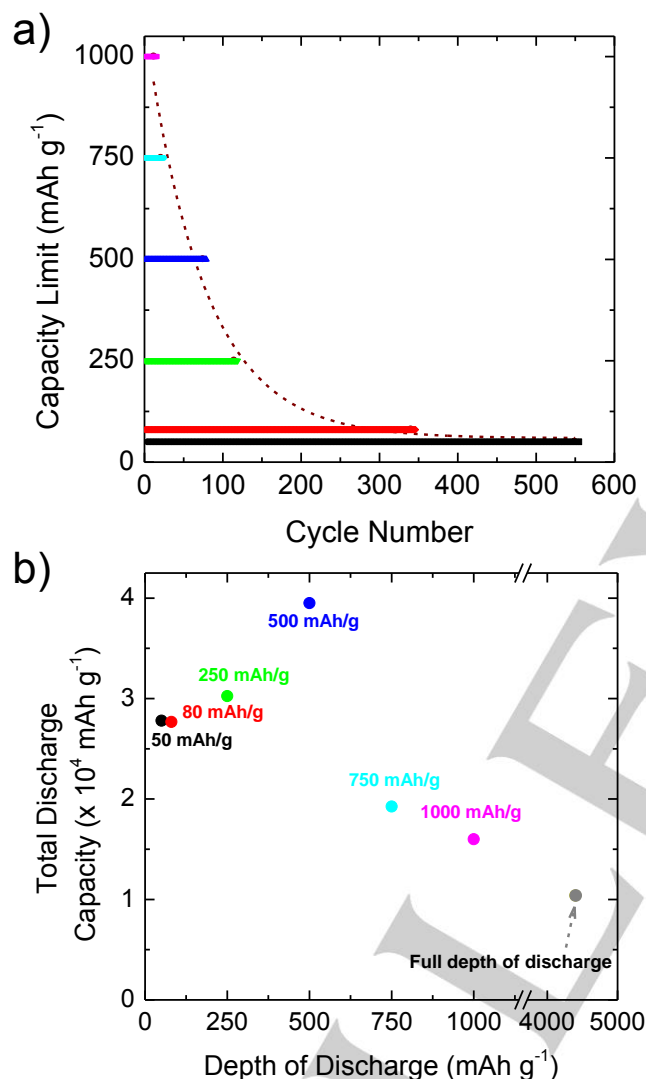

Figure 5. a) Cycle number as a function of capacity limit for symmetric cycling at 50 µA. b) Measured total capacity for the various depths of discharge investigated.

These results highlight the importance of depth of discharge in determining the total discharge capacity for other Li-O$_2$ battery systems. It is important to note that the commonly used 1000 mAhg^{-1} limit seen in the literature may represent a different actual % depth of discharge (i.e. 1000 mAhg^{-1} is 50% DOD for a cathode with a capacity of 2000 mAhg^{-1} but less than 10% DOD for some of the highest capacity cathodes reported in the literature[58]). Furthermore, while reducing depth of discharge will almost certainly increase the number of discharge cycles achievable (i.e. in Fig 5 b, a low capacity limit 50 mAhg^{-1} showed a remarkable cycle life of 556 cycles compared to just 79 cycles at 500 mAhg^{-1}, but a lower total cell capacity of 27,800 mAhg^{-1} compared to 39,500 mAhg^{-1} respectively, for coulombically equivalent cycles), the total discharge capacity may not increase linearly with decreasing depth of discharge. Furthermore, cycling stability (particularly at limited depth of discharge) is not necessarily an indication of true stability (i.e. reversible formation/decomposition of Li$_2$O$_2$).

We mapped the variation in the discharge-charge voltage inefficiencies (voltage gap, ∆E) during cycling for a series of depths of discharge, and also for symmetrically vs. asymmetrically discharged/charge cell cycling. Since the specific energy round trip efficiency is limited by the significant overpotential increase with respect to the discharge potential required to decompose the discharge products (among other high voltage effects), we quantified the benefit of the charging rate on cells discharged with each depth of discharge. Figure 6 a) plots the difference in the terminal charging overpotential against the final discharge potential at a limited discharge capacity of 1000 mAhg^{-1}. The three cells discharged at a current of 50 µA had the lowest voltage gap values and so the highest energy efficiency, and maintain the lowest voltage gap for a greater number of Coulombic efficiency cycles at the capacity limit of 1000 mAhg^{-1}. These cells also showed a much more gradual increase in voltage gap with each successive cycle than the tests discharged at 100 µA and 250 µA. Both cells discharged with a charge current of 250 µA (i.e. -100 µA /+250 µA and ±250 µA) possessed the highest voltage gaps of all the tests. This large voltage gap correlates with the extremely poor rechargeability of these Li-O$_2$ cells, and is fundamentally related to how the discharge products form at this faster rate during discharge. Limited product decomposition from fast discharge can be partially mitigated by recharging at a significantly slower rate for a specific capacity limit It can be seen that the last cycle for each of the tests (i.e. the last cycle at the desired capacity limit of 1000 mAhg^{-1}) exhibited a voltage gap between discharge and charge of ≥ 2.25 V.

Voltage gap analysis of cells with a 1000 mAg^{-1} depth of discharge symmetrically cycled at ± 50 µA in each case, was compared with similar tests at different depths of discharge (750 mAhg^{-1}, 500 mAhg^{-1}, 250 mAhg^{-1}, 80 mAhg^{-1} and 50 mAhg^{-1}) in Figure 6 b. The rate at which the voltage gap increases per cycle (a measure of reducing energy efficiency in the cell) is lowered as we reduced the depth of discharge. The rate increase of ∆E for the test at 500 mAhg^{-1} was markedly slower during initial cycles than all others, which may explain the large improvement in the total capacity at this depth of discharge as presented in Figure 5 – while lower depths of discharge also provide significant cycle life once the charging rate is slow, all cells that exhibit a fast increase in the voltage gap will have curtailed cycle life. The voltage gap data for the other depths of discharge (250 mAhg^{-1}, 80 mAhg^{-1} and 50 mAhg^{-1}) was limited to the first 100 cycles for clarity and showed a clear reduction in energy loss per cycle as the depth of discharge is decreased, thus extending the cycle life of the battery.
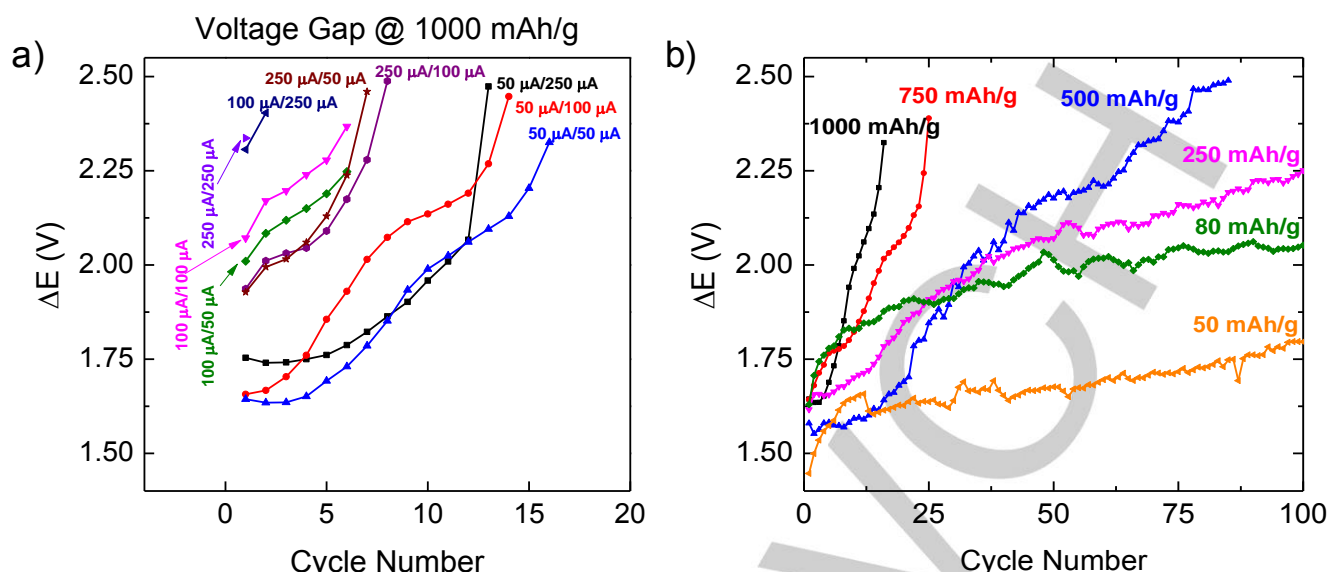
FULL PAPER

Figure 6. a) Voltage gaps (ΔE) between terminal voltages of discharge and charge for the various tests conducted at a fixed capacity of 1000 mAhg^{-1}. b) Voltage gaps between discharge and charge for different depths of discharge for symmetric cycling at 50 µA.

Conclusions

In conclusion, we have investigated the impact of depth of discharge and discharge/charge asymmetry on the cycle life of a high capacity cathode/electrolyte pairing for Li-O$_2$ batteries. While the best and worst cycle life values at a fixed capacity of 1000 mAhg^{-1} were seen at the lowest (± 50 µA) and highest (± 250 µA) symmetric applied current respectively as would be expected, it was found that asymmetric tests with a 250 µA discharge current but lower charge currents (50 µA or 100 µA) showed greatly improved cycle life compared to the symmetric high current case. Interestingly, it was found that discharging the cell with the lowest applied current of 50 µA meant that the cycle life was less sensitive to the subsequent charge current than for the higher discharge currents. The number of cycles achievable with a discharge current of 50 µA at the capacity limit of 1000 mAhg^{-1} was 16 (for 50 µA recharge), 14 (for 100 µA recharge) and 13 (for 250 µA recharge).

The impact of depth of discharge on determining the total cumulative discharge capacity was also investigated. This was done at a fixed symmetric discharge/charge current of 50 µA (which had previously shown the best cycle life at a depth of discharge of 1000 mAhg^{-1}). Tests conducted at full depth of discharge (i.e. cycled between 2 V- 4.5 V) showed a rapid drop off in capacity and a poor cycle life. Reducing the depth of discharge to 50 mAhg^{-1} led to a cycle life of 556 cycles (with a total discharge capacity of 27,800 mAhg^{-1}), however, the total cumulative discharge capacity in this case was actually highest for a depth of discharge of 500 mAhg^{-1} (39,500 mAhg^{-1}). These results suggest that ~10 % depth of discharge for this system allows for the highest total discharge capacity. This finding has implications for other cathode/electrolyte pairings and suggests that future reports should investigate the impact of depth of discharge on total (cumulative) discharge capacity and cycle life rather than with a fixed capacity limit. Fixed capacity limits may vary considerably as a % depth of discharge for different Li-O$_2$

systems (electrolytes, additives, binders, cathodes, catalysts etc.) Combining the approach of tailoring the depth of discharge with asymmetric discharge/charge rates (which also controls Li$_2$O$_2$ morphology) to suit desired applications may dramatically improve cycle life for a fixed system, or at least provide a means of gauging the cycling conditions that maximize cycle life at high efficiency for a fixed capacity limit. Given the numerous stability issues existing with Li-O$_2$ batteries, working within more stable system boundaries (e.g. limiting charge overpotentials by reducing charge rate) offers potential for Li-O$_2$ battery performance improvements until more stable electrolyte/cathode materials can be identified. This method can be applied to all Li-O$_2$ cells (or other reversible electrochemical systems) with new electrolytes and materials, especially with ORR or OER catalysts and under conditions where surface vs solution mediated peroxide growth affects the kinetics of reversible Li$_2$O$_2$ formation. The method can be adapted to compare to analytical techniques that probe parasitic reactions, to investigate the charge-discharge conditions that minimize the effect of parasitic reactions and other processes that influence cycle life and energy efficiency.

Experimental Section

Materials

LiTFSI (99.95 %), anhydrous DMSO (≥ 99 %) and multi-walled carbon nanotubes (outer diameter 10-15 nm, inner diameter 2-6 nm, length 0.1-10 µm) were purchased from Sigma Aldrich. LiTFSi was dried under vacuum at 80 °C overnight prior to use. Li chips were purchased from MTI. PEO was purchased from Polymer Source Inc. (average mw 97,000).

Cathode preparation

Cathodes were prepared by creating slurries of multi-walled carbon nanotubes and PEO binder in a weight ratio of 4.5:1 in NMP. The resultant

FULL PAPER

slurries were mechanically stirred before being dip coated on stainless steel mesh current collectors (diameter 1.76 cm^2). The meshes were dried overnight at 100 °C to remove the solvent and transferred immediately to a glovebox. The total mass loading on each of the cathodes was 0.7 ± 0.2 mg with all capacities calculated based on the mass of binder and carbon. All currents were applied as fixed currents (50, 100, and 250 µA). For example, this corresponds to specific currents of 142 mA/g ± 28.6 mA/g for the tests with applied currents of 100 µA.

Li-O$_2$ cell assembly and electrochemical characterization

Electrochemical tests were performed using an El-Cell split cell. All cells were constructed within an Ar filled glovebox (O$_2$ and H$_2$O < 0.1 ppm). Given the critical role of H$_2$O content in determining the electrochemical response, KF (Karl Fischer) analysis was performed on the DMSO electrolyte after preparation using a Metrohm 684 KF coulometer instrument. The water content of the electrolyte was found to be 98 ppm as we reported previously.[25] All cathodes were prepared on stainless steel mesh current collectors as described above. A glass fiber filter paper was used as separator upon which 100 µl of electrolyte was added. A Li chip (MTI) was polished on both sides and used as the anode. The cell was tightened and removed from the glovebox where it was immediately connected to an O$_2$ line and then purged with 0.25 bar O$_2$ for 60 minutes at open circuit voltage (OCV). Following this period, the O$_2$ flow was ceased and the oxygen inlet and outlet valves were closed. The cell was allowed to rest for another hour in this closed configuration. Electrochemical measurements were conducted using a VSP Biologic galvanostat. All galvanostatic measurements were conducted using fixed applied currents rather than currents calculated based on the mass of the cathode material. All voltages quoted are vs Li/Li$^+$. The total discharge capacity form a particular test was calculated from the product of cycle number and the fixed capacity limit.

Acknowledgements

[1] P. G. Bruce, S. A. Freunberger, L. J. Hardwick, J. M. Tarascon, *Nat. Mater.* **2011**, *11*, 19.
[2] P. G. Bruce, L. J. Hardwick, K. Abraham, *MRS Bull* **2011**, *36*, 506.
[3] G. Girishkumar, B. McCloskey, A. C. Luntz, S. Swanson, W. Wilcke, *J. Phys. Chem. Lett.* **2010**, *1*, 2193.
[4] A. C. Luntz, B. D. McCloskey, *Chem. Rev.* **2014**, *114*, 11721.
[5] M. D. Bhatt, H. Geaney, M. Nolan, C. O'Dwyer, *Phys. Chem. Chem. Phys.* **2014**, *16*, 12093.
[6] K. Abraham, Z. Jiang, *J. Electrochem. Soc.* **1996**, *143*, 1.
[7] B. D. McCloskey, A. Speidel, R. Scheffler, D. C. Miller, V. Viswanathan, J. S. Hummelshøj, J. K. Nørskov, A. C. Luntz, *J. Phys. Chem. Lett.* **2012**, *3*, 997.
[8] Y.-C. Lu, D. G. Kwabi, K. P. C. Yao, J. R. Harding, J. Zhou, L. Zuin, Y. Shao-Horn, *Energy Environ. Sci.* **2011**, *4*, 2999.
[9] B. D. McCloskey, D. S. Bethune, R. M. Shelby, G. Girishkumar, A. C. Luntz, *J. Phys. Chem. Lett.* **2011**, *2*, 1161.
[10] B. Horstmann, B. Gallant, R. Mitchell, W. G. Bessler, Y. Shao-Horn, M. Z. Bazant, *J. Phys. Chem. Lett.* **2013**, *4*, 4217.
[11] K. G. Gallagher, S. Goebel, T. Greszler, M. Mathias, W. Oelerich, D. Eroglu, V. Srinivasan, *Energy Environ. Sci.* **2014**, *7*, 1555.
[12] Z. Peng, S. A. Freunberger, Y. Chen, P. G. Bruce, *Science* **2012**, *337*, 563.
[13] M. M. O. Thotiyl, S. A. Freunberger, Z. Peng, Y. Chen, Z. Liu, P. G. Bruce, *Nat. Mater.* **2013**, *12*, 1049.
[14] K. U. Schwenke, M. Metzger, T. Restle, M. Piana, H. A. Gasteiger, *J. Electrochem. Soc.* **2015**, *162*, A573.
[15] T. Ogasawara, A. Débart, M. Holzapfel, P. Novák, P. G. Bruce, *J. Am. Chem. Soc.* **2006**, *128*, 1390.
[16] Y.-C. Lu, B. M. Gallant, D. G. Kwabi, J. R. Harding, R. R. Mitchell, M. S. Whittingham, Y. Shao-Horn, *Energy Environ. Sci.* **2013**, *6*, 750.
[17] J. Yang, D. Zhai, H.-H. Wang, K. C. Lau, J. A. Schlueter, P. Du, D. J. Myers, Y.-K. Sun, L. A. Curtiss, K. Amine, *Phys. Chem. Chem. Phys.* **2013**, *15*, 3764.
[18] D. Zheng, Q. Wang, H.-S. Lee, X.-Q. Yang, D. Qu, *Chem. Eur. J.* **2013**, *19*, 8679.
[19] M. Olivares-Marín, A. Sorrentino, R.-C. Lee, E. Pereiro, N.-L. Wu, D. Tonti, *Nano Lett.* **2015**, *15*, 6932.
[20] C. O. Laoire, S. Mukerjee, K. M. Abraham, E. J. Plichta, M. A. Hendrickson, *J. Phys. Chem. C* **2009**, *113*, 20127.
[21] C. Xia, M. Waletzko, L. Chen, K. Peppler, P. J. Klar, J. Janek, *ACS Appl. Mater. Interfaces* **2014**, *6*, 12083.
[22] S. Meini, N. Tsiouvaras, K. U. Schwenke, M. Piana, H. Beyer, L. Lange, H. A. Gasteiger, *Phys. Chem. Chem. Phys.* **2013**, *15*, 11478.
[23] Y. Hu, X. Han, F. Cheng, Q. Zhao, Z. Hu, J. Chen, *Nanoscale* **2014**, *6*, 177.
[24] N. B. Aetukuri, B. D. McCloskey, J. M. García, L. E. Krupp, V. Viswanathan, A. C. Luntz, *Nat. Chem.* **2015**, *7*, 50.
[25] H. Geaney, C. O'Dwyer, *J. Electrochem. Soc.* **2016**, *163*, A43.
[26] M. M. Ottakam Thotiyl, S. A. Freunberger, Z. Peng, P. G. Bruce, *J. Am. Chem. Soc.* **2013**, *135*, 494.
[27] S. A. Freunberger, Y. Chen, Z. Peng, J. M. Griffin, L. J. Hardwick, F. Bardé, P. Novák, P. G. Bruce, *J. Am. Chem. Soc.* **2011**, *133*, 8040.
[28] R. Black, S. H. Oh, J.-H. Lee, T. Yim, B. Adams, L. F. Nazar, *J. Am. Chem. Soc.* **2012**, *134*, 2902.
[29] Y.-C. Lu, E. J. Crumlin, G. M. Veith, J. R. Harding, E. Mutoro, L. Baggetto, N. J. Dudney, Z. Liu, Y. Shao-Horn, *Sci. Rep.* **2012**, *2*, 715.
[30] O. Oloniyo, S. Kumar, K. Scott, *J. Electron. Mater.* **2012**, *41*, 921.
[31] G. Wang, L. Huang, S. Liu, J. Xie, S. Zhang, P. Zhu, G. Cao, X. Zhao, *ACS Appl. Mater. Interfaces* **2015**, *7*, 23876.
[32] R. Choi, J. Jung, G.-B. Kim, K.-S. Song, Y. Kim, S. C. Jung, Y.-K. Han, H. Song, Y. Kang, *Energy Environ. Sci.* **2014**, *7*, 1362.
[33] H. Wang, Y. Yang, Y. Liang, G. Zheng, Y. Li, Y. Cui, H. Dai, *Energy Environ. Sci.* **2012**, *5*, 7931.
[34] J. Lu, Y. Lei, K. C. Lau, X. Luo, P. Du, J. Wen, R. S. Assary, U. Das, D. J. Miller, J. W. Elam, *Nat. Commun.* **2013**, *4*, 2383.
[35] P. Zhang, X. Lu, Y. Huang, J. Deng, L. Zhang, F. Ding, Z. Su, G. Wei, O. G. Schmidt, *J. Mater. Chem. A* **2015**, *3*, 14562.
[36] J. Lu, Y. Jung Lee, X. Luo, K. Chun Lau, M. Asadi, H.-H. Wang, S. Brombosz, J. Wen, D. Zhai, Z. Chen, D. J. Miller, Y. Sub Jeong, J.-B. Park, Z. Zak Fang, B. Kumar, A. Salehi-Khojin, Y.-K. Sun, L. A. Curtiss, K. Amine, *Nature* **2016**, *529*, 377.
[37] M. Noked, M. A. Schroeder, A. J. Pearse, G. W. Rubloff, S. B. Lee, *J. Phys. Chem. Lett.* **2016**, *7*, 211.
[38] Y.-C. Lu, Y. Shao-Horn, *J. Phys. Chem. C* **2012**, *4*, 93.
[39] J. Wang, H.-x. Zhong, Y.-l. Qin, X.-b. Zhang, *Angew. Chem. Int. Ed.* **2013**, *52*, 5248.
[40] S. Jee, W. Choi, C. H. Ahn, G. Yang, H. K. Cho, J.-H. Lee, C. Yu, *J. Mater. Chem. A* **2015**, *3*, 13767.
[41] B. D. Adams, C. Radtke, R. Black, M. L. Trudeau, K. Zaghib, L. F. Nazar, *Energy Environ. Sci.* **2013**, *6*, 1772.
[42] D. G. Kwabi, T. P. Batcho, C. V. Amanchukwu, N. Ortiz-Vitoriano, P. Hammond, C. V. Thompson, Y. Shao-Horn, *J. Phys. Chem. Lett.* **2014**, *5*, 2850.

FULL PAPER

[43]   M. A. Schroeder, N. Kumar, A. J. Pearse, C. Liu, S. B. Lee, G. W. Rubloff, K. Leung, M. Noked, *ACS Appl. Mater. Interfaces* **2015**, *7*, 22364.

[44]   D. Xu, Z.-l. Wang, J.-j. Xu, L.-l. Zhang, X.-b. Zhang, *Chem. Commun.* **2012**, *48*, 6948.

[45]   H.-D. Lim, K.-Y. Park, H. Song, E. Y. Jang, H. Gwon, J. Kim, Y. H. Kim, M. D. Lima, R. O. Robles, X. Lepró, R. H. Baughman, K. Kang, *Adv. Mater.* **2013**, *25*, 1348.

[46]   D. Sharon, M. Afri, M. Noked, A. Garsuch, A. A. Frimer, D. Aurbach, *J. Phys. Chem. Lett.* **2013**, *4*, 3115.

[47]   M. J. Trahan, S. Mukerjee, E. J. Plichta, M. A. Hendrickson, K. Abraham, *J. Electrochem. Soc.* **2013**, *160*, A259.

[48]   D. Sharon, D. Hirsberg, M. Afri, F. Chesneau, R. Lavi, A. A. Frimer, Y.-K. Sun, D. Aurbach, *ACS Appl. Mater. Interfaces* **2015**, *7*, 16590.

[49]   R. R. Mitchell, B. M. Gallant, C. V. Thompson, Y. Shao-Horn, *Energy Environ. Sci.* **2011**, *4*, 2952.

[50]   L. Zhong, R. R. Mitchell, Y. Liu, B. M. Gallant, C. V. Thompson, J. Y. Huang, S. X. Mao, Y. Shao-Horn, *Nano Lett.* **2013**, *13*, 2209.

[51]   Q.-C. Zhu, F.-H. Du, S.-M. Xu, Z.-K. Wang, K.-X. Wang, J.-S. Chen, *ACS Appl. Mater. Interfaces* **2016**, *8*, 3868.

[52]   K. R. Yoon, J.-W. Jung, I.-D. Kim, *ChemNanoMat* **2016**, *2*, 616.

[53]   C. V. Amanchukwu, J. R. Harding, Y. Shao-Horn, P. T. Hammond, *Chem. Mater.* **2014**, *27*, 550.

[54]   H. Geaney, J. O'Connell, J. D. Holmes, C. O'Dwyer, *J. Electrochem. Soc.* **2014**, *161*, A1964.

[55]   H. Geaney, C. O'Dwyer, *Phys. Chem. Chem. Phys.* **2015**, *17*, 6748

[56]   Y. Zhang, H. Zhang, J. Li, M. Wang, H. Nie, F. Zhang, *J. Power Sources* **2013**, *240*, 390.

[57]   E. J. Nemanick, R. P. Hickey, *J. Power Sources* **2014**, *252*, 248.

[58]   Z. L. Wang, D. Xu, J. J. Xu, L. L. Zhang, X. B. Zhang, *Adv. Funct. Mater.* **2012**, *22*, 3699.

[59]   B. Sun, X. Huang, S. Chen, P. Munroe, G. Wang, *Nano Lett.* **2014**, *14*, 3145.

[60]   M. Hong, H. C. Choi, H. R. Byon, *Chem. Mater.* **2015**, *27*, 2234.

WILEY-VCH

FULL PAPER

Entry for the Table of Contents (Please choose one layout)

Layout 1:

FULL PAPER

This work quantifies the influence of asymmetric charge-discharge operation of Li-O₂ battery cells and demonsrates the importance of appropriate discharge/charge rate and depth of discharge selection for directly improving cycle life performance of Li-O₂ batteries. Limiting the depth-of-discharge while unbalancing discharge/charge rate symmetry controls the total capacity to extend Li-O₂ battery cycle life, and predicts that cycle life at a fixed capacity limit.
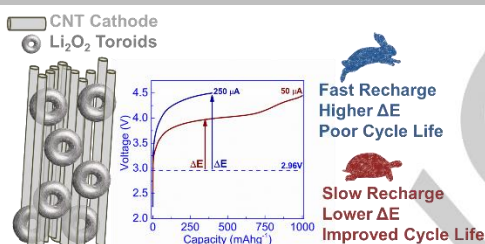
Hugh Geaney and Colm O'Dwyer*

Page No. – Page No.
Tailoring Asymmetric Discharge-Charge Rates and Capacity Limits to Extend Li-O₂ Battery Cycle Life